

We would like to thank both reviewers for their constructive feedback, which helped us to clarify the presented methods and improve the manuscript significantly.

Please find our response below, and all the changes in the revised manuscript (tracked changes).

Interactive comment on “Fast domain-aware neural network emulation of a planetary boundary layer parameterization in a numerical weather forecast model” by Jiali Wang et al.

Anonymous Referee #1

Received and published: 5 June 2019

This paper presents a series of neural networks designed to reproduce the output of the YSU PBL parameterization in the WRF model. The goal is to use the NN as a proxy model to reduce the computational cost of running the WRF model. The premise of the work is interesting and worthy of publication. There are several points of clarification and confusion however.

1. The topology of the models is confusing. The FFN is fine, but the size of the hidden layers should be noted. The two hierarchical models appear to be a series of nested single layer neural networks that output at each level. The goal is to enforce layer specificity, though I am not sure why this cannot also happen in the FFN as with what I assume are a larger number of internal weights and fully connected, it should be able to encode this information as well.

Response: In the revised manuscript, we detailed the figure description for Figure 1, which shows the architecture of each neural network. We specified that we have 17 hidden layers for all three neural network, indicated by the purple unit in Figure 1. We also revise the manuscript to further emphasize the difference between the three neural networks. The FFN takes all the output data (17 vertical WRF model layer \times 5 variables/layer) and input data for training. The training process doesn't know which data belongs to which layer, the output layer comprises 85 output variables. While this is a typical way to develop neural network, it doesn't consider any vertical mixing in a PBL profile. Therefore, we develop the other two neural networks, which has 17 output layers with each of them having 5 output variables for the particular PBL layer. Each of the 17 hidden layers uses the output from each of these output layers and also the near-surface input, and calculate the output for the next output layer. From the neural network perspective, the key advantage of HPC and HAC over FNN is effective back-propagation while training. In HPC and HAC, each hidden layer has an output layer; therefore, during the back propagation, the gradients from each of the output layer can be used to update the weights of the hidden layer directly to minimize the error for PBL layer specific outputs.

2. I don't understand why the FFN performance is so much worse. If the intermediate layers are sized large enough, then it should have a much larger number of connections and be able to encode more than the hierarchical models. It appears to cut out in training much earlier however. Is this just overfitting due to larger number of connections vs training data? If the amount of data was vastly increased, would we expect FFN to eventually overtake the performance of the hierarchical models?

Response: We clarified this issue and provided an explanation in the revised manuscript. As we mentioned in the response to your first comment, the FFN takes *all* the output data (17 vertical WRF model layers \times 5 variables per layer) and input data for training. The training process doesn't know which data belongs to which layer, the 85 variables are treated as a *whole thing*. The key advantage of HPC and HAC over FNN is that, during the training of HPC and HAC, because each of their hidden layer has an output layer, so during the back propagation, the gradients from each of the output layer can be used to update the weights of the hidden layer directly to minimize the error for that particular PBL layer. While for FFN, there is no output layers for each hidden layer, so there is no information that the backward propagation of FFN can take to update weights and minimize errors.

3. The writeup of the evaluation is a bit confusing. In particular L231-236. I assume it means that you trained using a single grid location, then applied the model to multiple grid points within 800km. If so this should be made more clear. Also why specify individual sites. One could calculate performance on all grid points within 800km. While doing this, it would be useful to see the drop off in performance as a function of distance. The last two plots start down this path, but with the density of points in a model, it should be straight forward to give performance as a function of distance from training point within the 800km range.

Response: Thanks for your suggestions. We have modified the text in line 231-236 to clarify that we trained our DNNs at a single location (e.g. Logan, Kansas) and then we apply the DNN to multiple grid points nearby. We also update the last two figures and the corresponding discussions. Instead of picking several stations, we test the DNN models over all the grid points of an 1100×1100 km area, with 90×91 grid points. To reduce the computing burden, we pick every other 7 grid points and get 13×13 grid points over the area, which still maintain the terrain height variability. Then we calculate RMSE and Pearson correlations of the neural network predictions compared with observations (here WRF model simulation), and see how RMSE and correlation change with distance from the center (where we develop the DNNs) of the 13×13 area. Results show that the neural network can be used by other locations if they are not far, and they have very similar terrain conditions for temperature, water vapor and wind speed. For wind direction, to use the same neural network, the nearby grid points should also under the same weather regimes, such as the large-scale circulations, etc. This indicates that, it's not always safe to train one model over a region unless the region has homogenous features in every regard we discussed here.

If we trained the network over a larger domain, we may need larger dataset for training. There is likely an optimum domain size over which a network would be useful. Therefore, we think that there may be a small number of region specific networks necessary for representing the PBL process for our entire model coverage of North American continent. The transferability tests described in the paper are one approach that we can use to determine the size of a single DNN model and its application extent. Developing DNNs for the whole region will require significantly larger computing resources. These ideas are beyond the scope of this study and will be explored in the future.

4. Can the authors comment on where they see this being put in an online model? It seems like the round trip to and from a GPU (IO) would cause a much bigger delay than just calculating the YSU parameterization in place. Offline this is not as much of a concern as all the data can be preloaded, but when there is a round trip at every model time step, it seems like the IO would become the predominant factor, and not the computation.

Response: We need GPUs for faster training. In a deployment scenario, as shown in several deep learning case studies, CPUs are enough for fast inference/prediction. In that case, we do not need GPUs and can avoid the data movement cost. Moreover, we are anticipating that the next HPC platforms that will be available will be 'accelerated' CPUs (e.g. the exascale systems at the DOE leadership computing facilities at Argonne National Laboratory and Oak Ridge Laboratory). The goal of the accelerated CPU architecture is to decrease the IO costs and make the GPU an integral part of the CPU design. The types of models we discuss here will be highly suitable for these machines.

5. I assume this is meant to be used as a proxy model for YSU when you are interested in fiddling with a different portion of the model and just want something "good enough" that is computationally cheap (For instance, you're examining microphysical parameterizations, and don't care about PBL explicitly). Is there a concern that the feedback loops with being off by as much as this NN is (up to 60% for some parameters, though much less for most) would cause the output from YSU and this model to diverge quite quickly when being run as a replacement for YSU? If so is this just meant to be a parallel option for a parameterization, or as a drop in for YSU?

Response: The expectation we have is that these types of DNN models could function as a drop-in replacement for existing parameterizations. We have trained the model with a limited amount of grid cells

as a proof of concept. Eventually, this model will be trained for all regions and conditions for the extensive simulation database we have. The goal is to develop DNN emulators for all the expensive parts of the model (radiation, microphysics, cumulus etc.) that would function as a high-spatial resolution ‘emulator’ of the model. Another possible path is to develop an emulator for the entire model disregarding each process (e.g. Scher, JGR 2019). We expect both paths to lead to the development of emulators that will be critical for generating larger ensemble of model simulations for uncertainty quantification in future climate projections.

Reference:

Scher, S.: Toward data-driven weather and climate forecasting: Approximating a simple general circulation model with deep learning. *Geophysical Research Letters*, 45, 12,616–12,622, 2018.

Anonymous Referee #2

Received and published: 6 June 2019

This is a very interesting work. To the best of my knowledge, the authors are the first researchers who applied machine learning techniques to PBL parameterization. Their results are thought-provoking. Of course, the final evaluation of the developed NN must be performed in parallel runs of WRF with the original PBL parameterization and with the developed NN. However, it is an issue for a separate paper. I believe that this paper should be accepted after some revision and clarifications.

General comments:

1. It is not clear from the text if the authors developed a NN emulation of the PBL parameterization. NN emulation has the same inputs (sometimes augmented by additional metadata) and the same outputs as the original (in this case YSU) parameterization. Is this the case for the presented study?

Response: The DNN developed here is an emulator in the sense that it is trained using the output from YSU scheme (not MYJ or MYNN PBL scheme). The inputs for our DNNs closely correspond to variables that are used as inputs to the YSU scheme in the WRF model.

2. Domain-aware NN is a confusing term. Which domain are the authors talking about (geographic domain, domain covered by inputs in the input space, etc.)? From the sentence in the paper: “a key drawback of the naïve FFN is that it does not consider the underlying PBL domain structure, such as the patterns that are locality specific and the vertical dependence between different vertical levels of each profile”, it can be concluded that it is about vertical correlations between different vertical levels. Probably “domain-aware” name is misplaced (see also comment 5).

Response: We have used the word “domain-aware” to mean subject expertise and the word “domain” to mean the domain of science rather than a geographical or spatial domain. Thus, one of the goals of this study is to show the importance of collaborations between data scientists and domain science experts. We first develop a neural network without any additional insights from a domain expert, such as local and nonlocal mixing in the vertical direction but purely driven by a knowledge of the key inputs to the YSU scheme. We then develop neural network that incorporate domain expertise, and we consider both the local and non-local mixing by taking into account the connection between one certain layer and the previous one layer (HPC) and the previous all layers (HAC) as well as the near-surface variable as inputs. This leads to a significant improvement of the prediction accuracy. We had an explanation of the use of domain-aware in the abstract; in the revised manuscript; we made an effort to further explain it by pointing the nonlocal mixing, which are vital for the PBL process to capture the turbulence in the lower troposphere.

As we respond to Reviewer #1, the FFN takes all the output data (17 vertical WRF model layer x 5 variables/layer) and input data for training. The training process doesn't know which data (among the 85 variables) belongs to which layer, the output layer of FFN consider all 85 variables as a whole thing. While this is a typical way to develop neural network, it doesn't consider any vertical mixing in a PBL layer. Therefore, we develop the other two neural networks, which have 17 output layers with each of them having 5 variables for the particular PBL layer. Each hidden layer uses the output from each of these output layers and also the near-surface input, and calculate the output for the next output layer. From the neural network perspective, the key advantage of HPC and HAC over FNN is effective back-propagation while training. In HPC and HAC, each hidden layer has an output layer; so during the back propagation, the gradients from each of the output layer can be used to update the weights of the hidden layer directly to minimize the error for PBL layer specific outputs.

In summary, we still keep the domain-aware term, but we clarified that the domain-aware is about considering local and non-local mixing in the PBL.

3. I cannot completely agree with the aforementioned (in comment 2) sentence from the paper. First, FFN does accounts for vertical correlations in profiles because all level components of profile are built from the same neurons of the previous hidden layer. Second, in this particular study, as is explained in the text, all outputs (including all vertical components of the same profile) are normalized independently, which significantly reduces the sensitivity of FFN (and any NN) to vertical correlations between levels. To preserve vertical dependencies, a profile should be normalized as a whole but not each component independently.

Response: In the revised manuscript, we made an efforts to clarify the difference between FFN and HAC/HPC in both text and Figure 1. As we response to your comment 2, FFN takes all the output data (17 vertical WRF model layer x 5 variables/layer) and input data for training. The training process doesn't know which data belongs to which layer, the 85 output variables are treated as a whole. So it doesn't consider any vertical correlations in the profile.

We apologize for any unclear text in the original manuscript. we normalize each output variable independently, not each vertical layer independently. In other words, we normalize the whole profile of each variable separately, because the values of the five output variables are in different scale (range of values). The normalization is done per output variable so that they all have the same scale. This is a common approach in NN training as it allows the back propagation to treat the errors equally. Note that for prediction, we apply inverse transformation and compute the prediction error (R^2 and RMSE) in the original scale.

4. The time length of data set to be used for training is not a valuable and universal characteristic. It depends on representativeness of data set, i.e. on how well the variety of atmospheric states is represented in the training set, or how well the domain of input space is sampled. For example, including in the training set more grid points would enrich it with new/different atmospheric states and made more representative. It may shorten the time length of data required for training.

Response: Thanks for your comment. Reviewer #1 also had a similar insight. We do agree that the neural network developed in this study based on the individual location (Logan, Kansas) likely will not be applicable universally. However, this model will have a region of applicability that can be tested using similar approach to those discussed in the manuscript. We may need several such networks to cover the entire model simulated region or train the DNN with data from the entire model simulated region. The later option as explained will need to performed on HPC systems and will be the target of our future research.

We agree that training more grid points (in space) would enrich the dataset, but it also have the risk of introducing more noise for the neural network, unless the regions is homogenous. This might be done over a very small region by taking several grid points but not a relatively large region. By homogenous we mean that different grid points should also under the same weather regimes, such as the large scale circulations, etc. The reason we say this is that, from our spatial transferability analysis, we found the neural network can be used for temperature, water vapor, and even wind speed over other locations as far as 500km, but for wind direction, the different grid points should also under the same circulation patterns (for example, if the wind is driven by terrain over one location, then the network doesn't apply to locations that are driven by large-scale circulations). On the other hand, we do see it is worthwhile to develop DNNs for the whole region instead of individual locations. As we mentioned in our discussion, however, this will require additional computational consideration on HPC and will be considered in the follow-on effort.

5. Most/all problems with applications to neighboring grid points can be alleviated or completely removed if all grid points (entire grid) are included in training set together with some metadata, i.e. if lat, lon, and the terrain conditions (elevation etc.) are included as additional inputs at each grid point. The NN trained in such a way I'd call "domain-aware NN".

Response: Thanks for the suggestion and we found it's very helpful. In our revised manuscript, for the last two figures, instead of picking several stations we test the DNN models over all the grids of a 1100x1100 km area, with 90x91 grid points over that area. To reduce the computing burden, we pick every other 7 grid points and get 13x13 grid points over the area, which still maintain the terrain height variability. Then we calculate RMSE and correlations of the neural network prediction compared with observations (here WRF model simulation), and see how RMSE and correlation change with distance from the center (where we develop the DNNs) of the 13x13 area.

As we respond to your comment 2, we use the word 'domain' in the sense of domain-science expertise and not spatial domain. In other words, our neural networks were not developed considering spatial domain factors, they were developed only based on individual locations. It is referred to domain knowledges about the PBL structure, specifically, the local and nonlocal mixing of turbulence in the lower troposphere.

Specific comments:

1. Is the sizes of the input and output layers are $16 + 85 = 101$? (= near-surface variables) and 85 (= 17 vertical levels _ 5 output variables).

Response: For FFN, we have an input layer, which has 16 near-surface variables; we have 17 hidden layers; and one output layer, which has 85 variables (5 variables for each of the 17 WRF vertical layer).

For HPC, we have 16 near-surface variables as one part of the input, and we also use the output (5 variables) of each previous hidden layer as input for the next hidden layer. We have 17 hidden layers, and 17 output layers. HAC is similar to HPC, but uses the output of ALL the previous hidden layer as input for the next hidden layer.

We have specified this in text and also added clarifications in the caption of Figure 1.

2. It is not clear from the text how 17-level profiles produced by NN are integrated with WRF profiles in total 38 level profiles?

Response: The middle and upper troposphere (all layers above the PBL) are considered fully resolved by the dynamics simulated by the WRF model. So the upper 21 layers will be still from the WRF model itself. There may be discontinuity between the 17th and the 18th layer (which are from NN and the WRF, respectively), and need to be smoothed. This will be future study when we implement the NNs into WRF.

3. How many hidden layers have different NNs that the authors use?

Response: we used 17 hidden layers for all three NNs developed in this study. We add this information in the revised manuscript. The hidden layers are represented by the purple unit in Figure 1.

4. How many trained parameters (NN weights) has each of these NNs?

Response: for FNN we have 10,693 trained parameters; for HPC we have 16,597 trained parameters, and for HAC we have 26,197 trained parameters.

5. How many records has the training set that is used?

Response: We have described this in data at line 120-125 in the original manuscript. in the revised manuscript we move this description to **2.3 Setup** as following:

“The 22-year data from the WRF simulation was partitioned into three parts: a training set consisting of 20 years (1984–2003) of 3-hourly data to train the NN; a development set (also called validation set) consisting of 1 year (2004) of 3-hourly data used to tune the algorithm's hyperparameters and to control overfitting (the situation where the trained network predicts well on the training data but not on the test data); and a test set consisting of 1 year of records (2005) for prediction and evaluations.”

6. Did not the authors try to train a shallow NN with the same number of weights as the best DNN has? Without all this information it is difficult to understand why NNs with different architectures perform so differently.

Response: as we explained earlier, the FFN takes all the output data (17 vertical WRF model layer x 5 variables/layer) and input data for training. The training process doesn't know which data belongs to which layer, the 85 variables are treated as a whole. While this is a typical way to develop neural network, it doesn't consider any vertical mixing in a PBL layer. Therefore, we develop the other two neural networks, which has 17 output layers with each of them having 5 variables for the particular PBL layer. Each hidden layer uses the output from each of these output layers and also the near-surface input, and calculate the output for the next output layer. From the neural network perspective, the key advantage of HPC and HAC over FNN is effective back-propagation while training. In HPC and HAC, each hidden layer has an output layer; consequently, during the back propagation, the gradients from each of the output layer can be used to update the weights of the hidden layer directly to minimize the error for PBL layer specific outputs.

Fast domain-aware neural network emulation of a planetary boundary layer parameterization in a numerical weather forecast model

¹Jiali Wang, ²Prasanna Balaprakash, and ¹Rao Kotamarthi*

¹Environmental Science Division, Argonne National Laboratory, 9700 South Cass Avenue, Lemont, IL 60439, USA

²Mathematics and Computer Science Division, Argonne National Laboratory, 9700 South Cass Avenue, Lemont, IL 60439, USA

Correspondence to: Rao Kotamarthi (vrkotamarthi@anl.gov)

Abstract. Parameterizations for physical processes in weather and climate models are computationally expensive. We use model output from a set of simulations performed using the Weather Research Forecast (WRF) model to train deep neural networks and evaluate whether trained models can provide an accurate alternative to the physics-based parameterizations. Specifically, we develop an emulator using deep neural networks for a planetary boundary layer (PBL) parameterization in the WRF model. PBL parameterizations are commonly used in atmospheric models to represent the diurnal variation of the formation and collapse of the atmospheric boundary layer—the lowest part of the atmosphere. The dynamics of the atmospheric boundary layer, mixing and turbulence, within the boundary layer, as well as velocity, temperature, and humidity profiles within the boundary layer are all critical for determining many of the physical processes in the atmosphere. PBL parameterizations are used to represent these processes that are usually unresolved in a typical numerical weather model that operates at horizontal spatial scales in the tens of kilometers. We demonstrate that a domain-aware deep neural network, which takes account of underlying domain structure that are locality specific (e.g., terrain, spatial dependence vertically nonlocal mixing between multiple vertical layers), can successfully simulate the vertical profiles within the boundary layer of velocities, temperature, and water vapor over the entire diurnal cycle. We then assess the spatial transferability of the domain-aware neural networks by using a trained model from one location to nearby locations. Results show that a single trained model from a location over the midwestern United States produces predictions of wind speed components, temperature, and water vapor profiles over the entire diurnal cycle and all nearby locations with similar terrain

32 [conditions](#) with [correlations higher than 0.9](#)~~errors less than a few percent~~ when compared with
33 the WRF simulations used as the training dataset.

34 **1 Introduction**

35 Model developers use approximations to represent the physical processes involved in climate and
36 weather that cannot be resolved at the spatial resolution of the model grids or in cases where the
37 phenomena are not fully understood (Williams, 2005). These approximations are referred to as
38 parameterizations (McFarlane, 2011). While these parameterizations are designed to be
39 computationally efficient, calculation of a model physics package still takes a good portion of the
40 total computational time. For example, in the community atmospheric model (CAM) developed
41 by National Center for Atmospheric Research (NCAR), with spatial resolution of approximately
42 300 km and 26 vertical levels, the physical parameterizations account for about 70% of the total
43 computational burden (Krasnopolsky and Fox-Rabinovitz, 2006). In the Weather Research
44 Forecast (WRF) model, with spatial resolution of tens of kilometers, time spent by physics is
45 approximately 40% of the computational burden. The input and output overhead is around 20%
46 of the computational time at low node count (100's) and can increase significantly at higher node
47 count as a percentage of the total wall-clock time.

48 An increasing need in the climate community is performing high spatial resolution simulations
49 ([grid spacing of 104](#) km or less~~grid spacing~~) and generating large ensembles of these
50 simulations in order to address uncertainty in the model projections and to assess risk and
51 vulnerability [due to climate variability at local scale](#). Developing process emulators (Leeds et al.,
52 2013; Lee et al., 2011) that can reduce the time spent in calculating the physical processes will
53 lead to much faster model simulations, enabling researchers to generate high spatial resolution
54 simulations and a large number of ensemble members.

55 A neural network (NN) is composed of multiple layers of simple computational modules, where
56 each module transforms its inputs to a nonlinear output. Given sufficient data, an appropriate NN
57 can model the underlying nonlinear functional relationship between inputs and outputs with
58 minimal human effort. During the past two decades, NN techniques have found a variety of
59 applications in atmospheric science. For example, Collins and Tossot (2015) developed an
60 artificial NN model by taking numerical weather prediction model (e.g., WRF) output as input to

61 predict thunderstorm occurrence within a few hundreds of square kilometers about 12 hours in
62 advance. Krasnopolsky et al. (2016) used NN techniques for filling the gaps in satellite
63 measurements of ocean color data. Scher (2018) used deep learning to emulate the complete
64 physics and dynamics of a simple general circulation model and indicated a potential capability
65 of weather forecasts using this NN-based emulator. Neural networks are particularly appealing
66 for emulations of model physics parameterizations in numerical weather and climate modeling,
67 where the goal is to find nonlinear functional relationship between inputs and outputs (Cybenko,
68 1989; Hornik, 1991; Chen and Chen, 1995a,b; Attali and Pagès, 1997). NN techniques can be
69 applied to weather and climate modeling in two ways. One approach involves developing new
70 parameterizations by using NNs. For example, Chevallier et al. (1998; 2000) developed a new
71 NN-based longwave radiation parameterization, NeuroFlux, which has been used operationally
72 in the European Centre for Medium-Range Weather Forecasts four-dimensional variational data
73 assimilation system. ~~and~~ NeuroFlux is found eight times faster than the previous
74 parameterization. Krasnopolsky et al. (2013) developed a stochastic convection parameterization
75 based on learning from data simulated by a cloud-resolving model, (CRM), initialized with and
76 forced by the observed meteorological data. The NN convection parameterization was tested in
77 the NCAR CAM and produced reasonable and promising results for the tropical Pacific region.
78 Jiang et al. (2018) developed a deep NN-based algorithm or parameterization to be used in the
79 WRF model to provide flow-dependent typhoon-induced sea surface temperature cooling.
80 Results based on four typhoon case studies showed that the algorithm reduced maximum wind
81 intensity error by 60–70% compared with using the WRF model. The other approach for
82 applying NN to weather and climate modeling is to emulate existing parameterizations in these
83 models. For example, Krasnopolsky et al. (2005) developed an NN-based emulator for imitating
84 an existing atmospheric longwave radiation parameterization for the NCAR CAM. They used
85 output from the CAM simulations with the original parameterization for the NN training. They
86 found the NN-based emulator was 50–80 times faster than the original parameterization and
87 produced almost identical results.

88 We study NN models to emulate existing physical parameterizations in atmospheric models.
89 Process emulators that can reproduce physics parameterization can ultimately lead to the
90 development of a faster model emulator that can operate at very high spatial resolution as
91 compared with most current model emulators that have tended to focus on simplified physics

92 (Kheshigi et al., 1999). Specifically, this study involves the design and development of a
93 domain-aware NN to emulate a PBL parameterization using 22-year-long output created by a set
94 of WRF simulations. To the best of our knowledge, we are among the first to apply deep neural
95 networks to the WRF model to explore the emulation of physics parameterizations. As far as we
96 know from the literature available at the time of this writing, the only application of NNs for
97 emulating the parameterizations in the WRF model is by Krasnopolsky et al. (2017). In their
98 study, a three-layer NN was trained to reproduce the behavior of the Thompson microphysics
99 (Thompson 2008) scheme in the WRF-ARW model. While we focus on learning the PBL
100 parameterization and developing domain-aware NN for emulation of PBL, the ultimate goal of
101 our on-going project is to build an NN-based algorithm to empirically understand the process in
102 the numerical weather/climate models that could be used to replace the physics parameterizations
103 that were derived from observational studies. This emulated model would be computationally
104 efficient, making the generation of large ensemble simulations feasible at very high
105 spatial/temporal resolutions with limited computational resources. The key objectives of this
106 study are to answer the following questions specifically for PBL parameterization emulation: (1)
107 What and how much data do we need to train the model? (2) What type of NN should we apply
108 for the PBL parameterization studied here? (3) Is the NN emulator accurate compared with the
109 original physical parameterization? This paper is organized as follows. Section 2 describes the
110 data and the neural network developed in this study. The efficacy of the neural network is
111 investigated in Section 3. Discussion and summary follow in Section 4.

112 **2 Data and Method**

113 **2.1 Data**

114 The data we use in this study is [22-year](#) output from the regional climate model WRF version
115 [3.3.1, driven by NCEP-R2 for the period 1984-2005](#). WRF is a fully compressible,
116 nonhydrostatic, regional numerical prediction system with proven suitability for a broad range of
117 applications. The WRF model configuration and evaluations are given by Wang and Kotamarthi
118 (2014). Covering all the troposphere are 38 vertical layers, between the surface to approximately
119 16 km (100 hPa). The lowest 17 layers cover from the surface to about 2 km above the ground.
120 The PBL parameterization we used for this WRF simulation is known as the YSU scheme
121 ([Yonsei University](#); Hong et al., 2006). The YSU scheme uses a nonlocal-mixing scheme with an

122 explicit treatment of entrainment at the top of the boundary layer and a first-order closure for the
123 Reynolds-averaged turbulence equations of momentum of air within the PBL.

124 ~~We use the output of the WRF model driven by NCEP-R2 for the period 1984–2005. The 22-~~
125 ~~year data was partitioned into three parts: a training set consisting of 20 years (1984–2003) of 3-~~
126 ~~hourly data to train the NN; a development set (also called validation set) consisting of 1 year~~
127 ~~(2004) of 3 hourly data used to tune the algorithm’s hyperparameters and to control overfitting~~
128 ~~(the situation where the trained network predicts well on the training data but not on the test~~
129 ~~data); and a test set consisting of 1 year of records (2005) for prediction and evaluations. The~~
130 goal of the work described here is to develop an NN-based parameterization [emulator](#) that can be
131 used to replace the PBL parameterization in the WRF model. Thus, we expect the NN submodel
132 to receive a set of inputs that are equivalent to the inputs provided to the YSU scheme at each
133 timestep. ~~However, a key difference in our approach is that the vertical profiles of various state~~
134 ~~variables are reconstructed by the NN using only the inputs (near surface variables and 700 hPa~~
135 ~~geostrophic winds).~~

136 Table 1 shows the architecture in terms of inputs and outputs used in our experiments. The inputs
137 are near-surface characteristics including 2-meter water vapor, ~~2-meter~~ [and](#) air temperature, 10-
138 meter zonal and meridional wind, ground heat flux, incoming shortwave radiation, incoming
139 longwave radiation, PBL height, sensible heat flux, latent heat flux, surface friction velocity,
140 ground [temperature](#), soil temperature at 2 m below the ground, soil moisture at 0–0.3cm below
141 the ground, and geostrophic wind component at 700 hPa. The outputs for the NN architecture are
142 the vertical profiles of the following [five](#) model prognostic and diagnostic fields: temperature,
143 water vapor mixing ratio, ~~and~~ zonal and meridional wind (including speed and direction), [as well](#)
144 [as vertical motions](#). In this study we develop an NN emulation of the PBL parameterization;
145 hence we focus only on predicting the profiles within the PBL, which is on average around 200
146 m and 400 m during the night and afternoon of winter, respectively, and around 400 m and 1300
147 m during the night and afternoon of summer, respectively, for the locations studied here. The
148 middle and upper troposphere (all layers above the PBL) are considered fully resolved by the
149 dynamics simulated by the model and hence not parameterized. Therefore, we do not consider
150 the levels above PBL height because (1) they carry no information about input/output functional
151 dependence that affects the PBL and (2) if not removed, they introduce additional noise in [the](#)

152 training. Specifically, we use the WRF output from the first 17 layers, which are within 1,900
153 meters and well cover the PBL.

154 **2.2 Deep neural networks for PBL parameterization emulation**

155 A class of machine learning approaches that is particularly suitable for emulation of PBL
156 parameterization is supervised learning. This approach models the relationship between the
157 outputs and independent input variables by using training data (x_i, y_i) , for $x_i \in T \subset D$, where T is
158 a set of training points, D is the full data set, and x_i and $y_i = f(x_i)$ are inputs and its corresponding
159 output y_i , respectively. The function f that maps the inputs to the outputs is typically unknown
160 and hard to derive analytically. The goal of the supervised learning approach is to find a
161 surrogate function h for f such that the difference between $f(x_i)$ and $h(x_i)$ is minimal for all $x_i \in T$.
162 Many supervised learning algorithms exist in the machine learning literature. ~~In this paper,~~
163 ~~we~~This study focuses on deep neural networks (DNNs).

164 DNNs are composed of an input layer, a series of hidden layers, and an output layer. The input
165 layer receives the input x_i , which is connected to the hidden layers. ~~neural layers: a stack of nodes~~
166 ~~organized in a hierarchical way to model a nonlinear function.~~ ~~Within each neural~~ hidden layer
167 ~~, nodes~~ receives inputs from the previous hidden neural layer (except the first hidden layer that is
168 connected to the input layer) ~~s~~ and perform certain nonlinear transformations through a system
169 of weighted connections and a nonlinear activation function on the received input values. The
170 last hidden layer is connected to the output layer from which the predicted values are obtained.
171 The training data is given to the DNN neural network through the input neural layer. ~~The last~~
172 ~~neural layer of the stack in the network is the output neural layer from which the predicted values~~
173 ~~are obtained.~~ The training procedure consists of modifying the weights of the connections in the
174 network to minimize a user-defined objective function that measures the prediction error of the
175 network. Each iteration of the training procedure comprises two phases: forward pass and
176 backward pass. ~~In~~ the forward pass, ~~consists of passing~~ the training data are passed to the
177 network and ~~computing~~ the prediction error is computed; in the backward pass, the gradients of
178 the error function with respect to all the weights in the network is computed and used to update
179 the weights in order to minimize the error. Once the entire dataset ~~is passed~~ both forward and
180 backward through the DNN neural network (with many iterations), one epoch is completed.

181 ~~We consider three variants of DNN (see below). We construct all of them using a neural block~~
182 ~~that comprises a dense neural layer with N nodes and a rectified linear activation function, where~~
183 ~~N is user-defined parameters.~~

184 **Naïve DNN:**

185 **Deep feed-forward neural network (FFN):** This is a fully connected feed-forward ~~DNN deep~~
186 ~~neural network~~ constructed as a sequence of K - ~~hidden layers~~ ~~neural blocks~~, where the input of
187 the i th ~~hidden layer neural block~~ is from $\{i-1\}$ th ~~hidden layer block~~ and the output of the i th
188 ~~hidden layer neural block~~ is given as the input of the $\{i+1\}$ th- ~~hidden layer~~ ~~neural block~~. The
189 sizes of the input and output neural layers are 16 (= near-surface variables) and 85 (= 17 vertical
190 levels \times 5 output variables). See Figure 1a for an illustration.

191 **Domain-aware DNN:**

192 While the FFN is a typical way of applying NN for finding the nonlinear relationship between
193 input and output, a key drawback ~~of the naïve FFN~~ is that it does not consider the underlying
194 PBL ~~domain~~ structure, such as ~~the patterns that are locality specific and~~ the vertical connection
195 dependence between different vertical levels within the PBL of each profile. In fact, the FFN does
196 not know which data (among the 85 variables) belongs to which vertical levels in a certain
197 profile. This is not typically needed for NNs in general and in fact is usually avoided because, for
198 classification and regression, one can find visual features regardless of their locations. For
199 example, a picture can be classified as a certain object even that object has never appeared in the
200 given location in the training set. In our case, however, the location is fixed and the profiles over
201 that location is distinguishable from other locations if they have different terrain conditions.
202 Consequently, we want it is desired to learn the particular influence of location vertical connection
203 between multiple layers within the PBL in the forecast. For example, the feature at a lower level
204 of a profile plays a role in the feature at a higher level and can help refine the output at the higher
205 level and accordingly the entire profile. This dependence may inform the NN and provide better
206 accuracy and data efficiency. To that end, we develop two variants of ~~domain-aware DNNs~~ for
207 PBL emulation.

208 **Hierarchically connected network with previous layer only connection (HPC):** We assume
209 that the outputs at each altitude level depend not only on the 16 near-surface variables but also

210 on the *adjacent* altitude level below it. To model this explicitly, we develop a ~~a domain-aware~~
211 DNN variant ~~in which~~ as follows: the input layer is connected to the first hidden layer followed
212 by the output layer of size 5 (five variable at each layer: temperature, water vapor, zonal and
213 meridional wind, and vertical motions) that corresponds to the first PBL ~~layer~~. This output layer
214 along with the input layer is connected to second hidden layer, which is connected to the second
215 output layer of size 5 that corresponds to the second PBL ~~layer~~. Thus, the input to an i th hidden
216 layer comprises the input layer of the 16 near-surface variables and the $(i-1)$ th output layer below
217 it ~~17 neural blocks are connected as follows: the input to an i th ($i > 1$) neural block comprises the~~
218 ~~input neural layer of the 16 near surface variables and the 5 outputs of the $(i-1)$ th neural block.~~
219 The first neural block, which is next to the input layer, receives inputs only from the input neural
220 layer of the 16 near-surface variables. See Figure 1b for an example.

221 **Hierarchically connected network with all previous layers connection (HAC):** We assume
222 that the outputs at each PBL depend not only on the 16 near-surface variables but also on *all*
223 altitude levels below it. ~~To model this explicitly, we modify HPC DNN as follows: t~~The input to
224 an i th ~~hidden layer neural block~~ comprises the input ~~neural~~ layer of the 16 near-surface variables
225 and *all* output ~~layers s of the~~ $\{1, 2, \dots, i-1\}$ ~~neural blocks~~ below it. See Figure 1c for an example.

226 ~~From the physical process perspective, FNN, HPC, and HAC considers both local and non-local~~
227 ~~mixing processes within the PBL by taking into account not only the connection between a given~~
228 ~~point and its adjacent point (local mixing), but also the connections from multiple vertical~~
229 ~~altitude levels (e.g., surface and all the points that below the given points). Compared with solely~~
230 ~~local mixing process, non-local mixing process is showed to perform more accurately in~~
231 ~~simulating deeper mixing within an unstable PBL (Cohen et al. 2015). are inspired by K-~~
232 ~~Diffusion, hybrid and non-local mixing model hypothesis. [Rao, Jiali: Fill this]~~

233 ~~From the neural network perspective, the key advantage of HPC and HAC over FNN is effective~~
234 ~~back-propagation while training. In HPC and HAC, each hidden layer has an output layer;~~
235 ~~consequently, during the back propagation, the gradients from each of the output layer can be~~
236 ~~used to update the weights of the hidden layer directly to minimize the error for PBL ~~layer~~~~
237 ~~specific outputs.~~

238 2.3 Setup

239 For preprocessing, we applied StandardScaler (removes the mean and scales each variable to unit
240 variance) and MinMaxScaler (scales each variable between 0 and 1) transformations before
241 training, and we applied the inverse transformation after prediction so that the evaluation metrics
242 are computed on the original scale.

243 We note that there is no default value for N ~~units nodes~~ in a dense ~~hidden neural~~ layer. We
244 conducted an experimental study on FFN and found that setting N to 16 results in good
245 predictions. Therefore, we used the same value of $N = 16$ in HPC and HAC.

246 For the implementation of DNN, we used Keras (version 2.0.8), a high-level neural network
247 Python library that runs on the top of the TensorFlow library (version 1.3.0). We used the scikit-
248 learn library (version 0.19.0) for the preprocessing module. The experiments were run on a
249 Python (Intel distribution, version 3.6.3) environment.

250 All three DNNs used the following setup for training: optimizer = adam, learning rate = 0.001,
251 epochs = 1000, batch size = 64. Note that batch size and number of epochs define the number of
252 randomly sampled training points required before updating the model parameters and the number
253 times that training will work through the entire training dataset. To avoid overfitting issues in
254 DNNs, we use an early stopping criterion in which the training stops when the validation error
255 does not reduce for 10 subsequent epochs.

256 [The 22-year data from the WRF simulation was partitioned into three parts: a training set](#)
257 [consisting of 20 years \(1984–2003\) of 3-hourly data to train the NN; a development set \(also](#)
258 [called validation set\) consisting of 1 year \(2004\) of 3-hourly data used to tune the algorithm’s](#)
259 [hyperparameters and to control overfitting \(the situation where the trained network predicts well](#)
260 [on the training data but not on the test data\); and a test set consisting of 1 year of records \(2005\)](#)
261 [for prediction and evaluations.](#)

262 We ran training and inference on a NVIDIA DGX-1 platform: Dual 20-Core Intel Xeon E5-2698
263 v4 2.2 GHz processor with 8 NVIDIA P100 GPUs with 512 GB of memory. The DNN’s training
264 and inference leveraged only a single GPU.

265 **3 Results**

266 In the following discussion we evaluate the efficacy of the three DNNs by comparing their
267 prediction results with WRF model simulations. We refer to the results of WRF model
268 simulations as observations because the DNN learns all the knowledge from the WRF model
269 output, not from in situ measurements. We refer to the values from the DNN models as
270 predictions. We initiate our DNN development at one grid cell from WRF output that is close to
271 a site in the midwestern United States (Logan, Kansas, latitude= 38.8701°N; longitude=
272 100.9627°W) and another grid cell at a site in Alaska (Kenai Peninsula Borough, AK, latitude=
273 60.7237 °N; longitude=150.4484 °W) to evaluate the robustness of the developed DNNs. We
274 then apply our DNNs to an area with size of stations within ~11800 km x 1100 km, centered
275 at~~from~~ the Logan site to assess the spatial transferability of the DNNs. In other words, we train
276 our DNNs using a single location, and then apply the DNNs to multiple grid points nearby.
277 While the Alaska site has different vertical profiles, especially for wind directions, and lower
278 PBL heights in both January and July, the conclusion in terms of the model performance is
279 similar to the site over Logan, Kansas.

280 **3.1 DNN performance in temperature and water vapor**

281 Figure 2 shows the diurnal variation (explicitly 3 PM and 12 AM local time at Logan, Kansas) of
282 temperature and water vapor mixing ratio vertical profiles in the first 17 layers from the
283 observation and three DNN model predictions. ~~The 17 layers are within 1,900 meters and well~~
284 ~~cover the PBL.~~ The figures present results for both January and July of 2005. The dashed lines
285 show the lowest and highest (5th and 95th percentile, respectively) PBL heights for that particular
286 time. In general, the DNNs are able to produce similar shapes of the observed profiles, especially
287 within the PBL. Both the temperature and water vapor mixing ratio are lower in January and
288 higher in July. Within the PBL, the temperature and water vapor do not change much with
289 height; above the PBL to the entrainment zone, the temperature and water vapor start decreasing.
290 Among the three DNNs, HAC and HPC show very low bias and high accuracy in the PBL; ~~but~~
291 the FFN shows a relatively large discrepancy from the observation. Figure 3 shows the root-
292 mean-square error (RMSE) and Pearson correlation coefficient (COR) between observation and
293 three DNN predictions in the afternoon and midnight of January and July. The RMSE and COR
294 consider not only the time series of observation and prediction but also their vertical profiles
295 below the PBL heights for each particular time. Among the three DNNs, HPC and HAC always

296 show better skill with smaller RMSEs and higher CORs than does FFN. The reason is that the
297 FFN uses only the 16 near-surface variables as inputs and all the 85 variables (17 layers \times 5
298 variables/layer) as output, and does not have the knowledge about the vertical
299 connections~~consider dependence~~ between each of the vertical levels. In contrast, HPC and HAC
300 use ~~not only both~~ the near-surface variables ~~but also~~and the five output variables of one previous
301 vertical level (HPC) or all previous vertical levels (HAC) as inputs for predicting a certain
302 vertical level~~the profiles~~ of each field. This architecture is helpful for reducing errors of each
303 hidden layer during the backward propagation. ~~This approach~~It is also important because PBL
304 parameterizations are used to represent the vertical ~~dependence of these variables~~mixing of heat,
305 moist, and momentum within the PBL and this mixing can be across a larger scale than just the
306 adjacent altitude levels. ~~and are~~This process is usually unresolved in a typical climate and
307 weather models that operate at horizontal spatial scales in the tens of kilometers. ~~Compared with~~
308 ~~HAC, HPC sometimes shows slightly better accuracy with smaller RMSEs and higher CORs, but~~
309 ~~in other cases HPC performs similar to HAC.~~ These results indicate that the information from all
310 previous levels is not as important as information from the previous layer right below the
311 predicted layer. We find in general HAC and HPC perform similarly, although in winter
312 especially midnight when the PBL is shallow, the RMSE of temperature predicted by HAC is
313 larger than that predicted by HPC. In contrast, in summer especially in afternoon when the PBL
314 is deep, the RMSE of temperature predicted by HAC is smaller than that predicted by HPC. This
315 emphasizes the importance of consideration of multi-level vertical connection for deep PBL case
316 in the DNNs.

317 **3.2 DNN performance in wind component**

318 Figure 4 shows the diurnal variation of zonal and meridional wind (including wind speed and
319 direction) profiles in January and July 2005 from observation and three DNN predictions.
320 Compared with the temperature and water vapor profiles, the wind profiles are more difficult to
321 predict, especially for days (e.g., summer) that have a higher PBL. The wind direction does not
322 change much below the majority of the PBL, and it turns to westerly winds when going up and
323 beyond the PBL. The DNN prediction has difficulty predicting the profile above the PBL height,
324 as is expected because these layers are considered fully resolved by the dynamics simulated by
325 the WRF model and hence not parameterized. Therefore, we do not consider DNN performance

326 at the levels above PBL height, because the DNNs carry no information about input/output
327 functional dependence that affects the PBL. The wind speed increases with height in both
328 January and July within the PBL. Above the PBL heights, the wind speed still increases in
329 January but decreases in July. The reason is that in January the zonal wind, especially westerly
330 wind, is dominant in the atmosphere and the wind speed increases with height; in July, however,
331 the zonal wind is relatively weak, and the meridional wind is dominant with southerly wind
332 below ~2 km and northerly wind above 2 km. The decrease in wind speed above the PBL is just
333 about the transition of wind direction from southerly to northerly wind. Figure 5 shows the
334 RMSEs and CORs between the observed and predicted wind component within the PBL. The
335 wind component is fairly well predicted ~~especially~~ by the HAC and HPC networks with
336 correlation above 0.8 for wind speed and 0.7 for wind direction except in July at midnight, which
337 is ~~below near 0.5 zero~~. Similar to the predictions for temperature and water vapor, the FFN shows
338 the poorest prediction accuracy with large RMSEs and low CORs, especially for wind direction
339 in July midnight, the COR is below zero. For accurately predicting the wind direction, we found
340 that using the geostrophic wind at 700 hPa as one of the inputs for the DNNs is important.

341 **3.3 DNN dependence on length of training period**

342 Next, we evaluate how sensitive the DNN is to the amount of available training data and how
343 much data one would need in order to train a DNN. While we present Figures 2–5 using 20-year
344 (1984–2003) training data, here we gradually decrease the length of the training set to 12 (1992–
345 2003), 6 (1998–2003), 2 (2002–2003) years, and 1 (2003) year. The validation data (for tuning
346 hyper-parameters and controlling overfit) and the test data (for prediction) are kept the same as
347 in our standard training dataset, which is year 2004 and 2005, respectively. Figures 6 and 7 show
348 the RMSE and CORs between observed and predicted profiles of temperature, water vapor, and
349 wind component for January ~~and July at their local~~ midnight. Overall, the FFN network depends
350 heavily on the length of training dataset. For example, the RMSE of FFN predicted temperature
351 decreases from 7.2 K using one year of training data to 3.0 K using 20-year training data. HAC
352 and HPC also depend on the length of training data especially when less than 6-year training data
353 is available, but even their worst prediction accuracy (using one year of training data) is still
354 better than FFN using 20-year training data. The RMSEs of HPC and HAC predicted
355 temperature decrease from ~2.4 K using 1 year of training data to ~1.5 K using 20 years of

356 training data. The CORs of FFN predicted temperature increase from 0.73 using one year of
357 training data to 0.92 using 20 years of training data. The CORs for HPC and HAC increase
358 slightly with more training data, but overall they are above 0.85 using one year to 20 years of
359 training data.

360 Regarding the question about how much data one would need to train a DDN, for FFN, at least
361 from this study, the performance is not stable until one has 12 or more years of training data,
362 which is significantly better than having only 6 years or less of training data. For HAC and HPC,
363 however, having 6 years of training data seems sufficient to show a stable prediction. Increasing
364 the amount of training data shows only marginal improvement in predictive accuracy. In fact, in
365 contrast to HAC and HPC, the performance of FFN has not reached a plateau even with the 20
366 years of training data. This suggests that with longer training sets the predicting skill of ~~an even~~
367 ~~naïve approach like~~ FFN could be further improved even though it does not explicitly consider
368 the physical process within a PBL and eventually reach the accuracy of HAC and HPC using 6 or
369 more years of training data.

370 **3.4 DNN performance for nearby stlocations**

371 This section assesses the spatial transferability of the domain-aware neural networks (specifically
372 HAC and HPC) by using a trained model from one location (at Logan, Kansas, as presented
373 above) to other locations within an area with size of 11800 km x 1100 km, covering latitude from
374 33.431 to 44.086°N, and longitude from 107.418 to 93.6975°W, centered at kilometers from the
375 Logan site with different terrain ~~conditions~~ and vegetation conditions (Figure 8, top) types. To
376 reduce the computational burden, we pick every other 7 grid points in this area and use the 13 ×
377 13 grid points (which can still capture the terrain variability) to test the spatial transferability of
378 the DNNs developed based on the single location at Logan, Kansas. We choose ten locations, as
379 shown in Figure 8, among which two (Sites 1 and 2) are 300 km away from the Logan site; three
380 (Sites 3, 4, and 5) are 430 km away from the Logan site; and five (Sites 6 to 10) are 450–800 km
381 away from the Logan site, with Sites 9 and 10 the furthest and having the most different
382 elevations from the Logan site. For each of the 13× 13 grid points, we calculate the differences
383 and correlations between observations and predictions. Different from the preceding section,
384 here we calculate normalized RMSEs relative to each grid point site's observations averaged
385 over a particular time period, in order to make the comparison feasible between different grid

386 points over the areasites. As shown in Figures 8 and 9 and 10 by the normalized RMSEs and
387 Pearson correlations, in general, for temperature, water vapor, and wind speed, the neural
388 network still work fairly well for surrounding locations and even far locations with similar
389 terrain height, except over the grid points where the terrain height is much higher than the Logan
390 site, and the prediction skill gets worse with larger RMSEs. This suggests the DNNs developed
391 based on Logan site are not applicable for these locations. However, for wind direction, the
392 prediction skill is good over the western part of the tested area, but is not so good over the far
393 eastern part of the area. One of the reasons is perhaps because that the driver of the wind
394 direction over the western and the eastern part of the area are different (complex terrain versus
395 large-scale system). ~~when going farther from Logan site, where our domain-aware neural~~
396 ~~networks (HPC and HAC) were developed, the prediction skill either does not change or gets~~
397 ~~slightly worse depending on the locations and the difference in terrain conditions between the~~
398 ~~reference site (Logan, Kansas) and the remote sites (S1 to S10 in Figure 8). For example, the~~
399 ~~RMSEs for wind direction over Sites 2, 4, and 8 are similar to that over the Logan site. However,~~
400 ~~the RMSEs over the other sites, which have different elevations (either higher or lower) than that~~
401 ~~for Logan site, are much larger, suggesting the DNNs developed based on Logan site are not~~
402 ~~applicable for these locations.~~ Overall, These results indicate that, at least for this study, as long
403 as the terrain conditions (slope, elevation, and orientation) are similar, the DNNs developed
404 based on one single location can be applied with similar prediction skill for locations that are as
405 far as 520 km (equal to more than 40 grid cells in the WRF output used in this study) to predict
406 the ~~wind and also other~~ variables assessed in this study. The results also suggest that when
407 implementing the NN-based algorithm into the WRF model, if a number of grid cells are over a
408 homogenous region, one may not need to train the NN over every grid cell. This will
409 significantly save computing time because the training process takes the majority of the
410 computing resource (see below). ~~Similar to Figure 6, we see that the HPC network works better~~
411 ~~than HAC especially for temperature and water vapor over all the sites and for wind component~~
412 ~~over most of the sites examined here, indicating that the input from all previous layers is not as~~
413 ~~important as that from the input from only the layer next to the predicted layer.~~ While we show
414 results predicted by HAC in January here, we find similar conclusion from HPC prediction and
415 both HAC and HPC predictions in July, expect that the prediction skills are even better in July
416 for the adjacent locations.

417 **3.5 DNN training and prediction time**

418 Table 2 shows the number of epochs and time required for training FNN, HPC, and HAC for
419 various numbers of training years. Because of the early stopping criterion, the number of training
420 epochs performed by different methods is not same. Despite setting the maximum epochs to
421 1,000, all these methods terminate within 178 epochs. We observed that HPC performs more
422 training epochs than do FNN and HAC: given the same optimizer and learning rate for all the
423 methods, HPC has a better learning capability because it can improve the validation error more
424 than HAC and FNN can. For a given set of training data, the difference in the training time per
425 epoch can be attributed to the number of trainable parameters in FNN, HPC, and HAC (10,693,
426 16,597, and 26,197, respectively). As we increase the size of training data, the training time per
427 epoch increases significantly for all three DNN models. The increase also depends on the
428 number of parameters in the model. For example, increasing the training data from 1 year to 20
429 years increases the training time per epoch from 1.4 seconds to 11.4 seconds for FNN, from 1.1
430 seconds to 17.4 seconds, and from 1.4 seconds to 19.6 seconds for HPC and HAC, respectively.

431 The prediction times of FNN, HPC, and HAC are within 0.5 seconds for one-year data, making
432 these models promising for PBL emulation deployment. The difference in the prediction time
433 between models can be attributed to the number of parameters in the DNNs: the larger the
434 number of parameters, the [higher-longer](#) the prediction time. For example, the prediction times
435 for FNN are below 0.2 seconds when using different numbers of years for training, while those
436 for HAC are around 0.4 seconds. Despite the difference in the number of training years, the
437 number of parameters for a given model is fixed. Therefore, once the model is trained, the DNN
438 prediction time depends only on the model and the number of points in the test data (1 year in
439 this study). Theoretically, for the given model and the test data, the prediction time should be
440 constant even with different amounts of training dataset. However, we observed slight variations
441 in the prediction times that range from 0.17 to 0.29 seconds for FNN, 0.30 to 0.34 seconds for
442 HPC, and 0.36 to 0.42 seconds for HAC, which can be attributed to the system software.

443 **4 Summary and Discussion**

444 This study developed DNNs for emulating [atthe YSU](#) PBL parameterization that is used by the
445 WRF model. Two of the DDNs take into account the domain-specific features [\(e.g., nonlocal](#)

446 ~~mixing in terms of such as spatial/vertical~~ dependence ~~between multiple PBL layers in the vertical~~
447 ~~direction over the location where we develop the DNNs~~. The input and output data for the DNNs
448 are taken from a set of 22-year-long WRF simulations. We developed the DNNs based on a
449 midwestern location in the United States. We found that the domain-aware DNNs can reproduce
450 the vertical profiles of wind, temperature, and water vapor mixing ratio with high accuracy yet
451 require fewer data than the traditional DNN, which does not care about the domain-specific
452 features. The training process takes the majority of the computing time. Once trained, the model
453 can quickly predict the variables with decent accuracy. This ability makes the deep neural
454 network appealing for parameterization emulator.

455 Following the same architecture that we ~~applied~~ developed for Logan, Kansas, we also built DNNs
456 for one location at Alaska. The results share the same conclusion as we have seen for the Logan
457 site. For example, among the three DNNs, HPC and HAC show much better skill with smaller
458 RMSEs and higher correlations than does FFN. The wind profiles are more difficult to predict
459 than the profiles of temperature and water vapor. For FFN, the prediction accuracy increases
460 with more training data; for HPC and HAC, the prediction skill stays similar when having six or
461 more years of training data.

462 While we trained our DNNs over individual locations in this study using only one computing
463 node (with multiple processors), there are 300,000 grid cells over our WRF model domain,
464 which simulated the North American continent as a horizontal resolution of 12 km. To train a
465 model for all the grid cells or all the homogeneous regions over this large domain, we will need
466 to scale up the algorithm to hundreds if not thousands of computing nodes to accelerate the
467 training time and the make the entire NN-based simulation faster than the original
468 parameterization.

469 The ultimate goal of this project is to build an NN-based algorithm to empirically understand the
470 process in the numerical weather and climate models and to replace the PBL parameterization
471 and other time-consuming parameterizations that were derived from observational studies. ~~This~~
472 ~~emulated model thus would be computationally efficient and enable researchers to generate large~~
473 ~~ensemble simulations at very high spatial/temporal resolutions with limited computational~~
474 ~~resources~~. The DNNs developed in this study can provide numerically efficient solutions to a

475 wide range of problems in environmental numerical models where lengthy, complicated
476 calculations describing physical processes must be repeated frequently or need a large ensemble
477 of simulations to represent uncertainty. A possible future direction for this research is
478 implementing these NN-based schemes in WRF for a new generation of hybrid regional-scale
479 weather/climate models that fully represent the physics at a very high spatial resolution at a fast
480 computational time so as to provide the means for generating large ensemble model runs.

481 *Data and code availability.* The data used and the code developed in this study are available at
482 <https://github.com/pbalapra/dl-pbl>.

483 *Author contributions.* JW participated in the entire project by providing domain expertise and
484 analyzing the results from the NN-based emulator. PB developed the deep neural networks and
485 ~~did all~~conducted the experiments ~~presented in this study~~. RK proposed the idea of this project
486 and provided high-level guidance and insight for the entire study.

487 *Competing interests.* The authors declare that they have no conflict of interest.

488 *Acknowledgments.* The WRF model output was developed through computational support by the
489 Argonne National Laboratory Computing Resource Center and Argonne Leadership Computing
490 Facility. This material is based upon work supported by the U.S. Department of Energy, Office
491 of Science, under contract DE-AC02-06CH11357.

492 **References**

493 Attali, J. G., and Pagès, G.: Approximations of functions by a multilayer perception: A new
494 approach, *Neural Networks*, 6, 1069–1081, 1997.

495
496 Chevallier, F., Chéruy, F., Scott, N. A., and Chédin, A.: A neural network approach for a fast and
497 accurate computation of longwave radiative budget, *J. Appl. Meteorol.*, 37, 1385–1397, 1998.

498
499 Chen, T., and Chen, H.: Approximation capability to functions of several variables, nonlinear
500 functionals and operators by radial basis function neural networks, *Neural Networks*, 6, 904–
501 910, 1995a.

502

503 Chen, T., and Chen, H.: Universal approximation to nonlinear operators by neural networks with
504 arbitrary activation function and its application to dynamical systems, *Neural Networks*, 6, 911–
505 917, 1995b.

506
507 Chevallier, F., Morcrette, J.-J., Chéruy, F., and Scott, N. A.: Use of a neural-network-based
508 longwave radiative transfer scheme in the EMCWF atmospheric model, *Q. J. R. Meteorol. Soc.*,
509 126, 761–776, 2000.

510
511 Collins, W., and Tissot, P.: An artificial neural network model to predict thunderstorms within
512 400 km² South Texas domains, *Meteorol. Appl.*, 22 (3), 650-665, 2015.

513
514 [Cohen, A.E., Cavallo, S.M., Coniglio, M.C., Brooks, H.E.: A review of planetary boundary layer](#)
515 [parameterization schemes and their sensitivity in simulating a southeast U.S. cold season severe](#)
516 [weather environment, *Weather Forecast.*, 30, 591-612, 2015.](#)

517
518 Cybenko, G.: Approximation by superposition of sigmoidal functions, *Math. Control Signals*
519 *Syst.*, 2, 303–314, 1989.

520
521 Hauser, A., and Bühlmann, P.: Characterization and greedy learning of interventional Markov
522 equivalence classes of directed acyclic graphs. *J. Mach. Learn. Res.*, 13, 2409–2464, 2002.

523
524 Hong, S.-Y., Noh, S.Y., and Dudhia, J.: A new vertical diffusion package with an explicit
525 treatment of entrainment processes. *Mon. Wea. Rev.*, 134, 2318–2341, 2006.

526
527 Hornik, K.: Approximation capabilities of multilayer feedforward network, *Neural Networks*, 4,
528 251–257, 1991.

529
530 Jiang, G.-Q., Xu, J., and Wei, J.: A deep learning algorithm of neural network for the
531 parameterization of typhoon-ocean feedback in typhoon forecast models, *Geophysical Research*
532 *Letters*, 45, 3706–3716, 2018.

533

534 Kheshgi, H. S., Jain, A. K., Kotamarthi, V. R., and Wuebbles, D. J.: Future atmospheric methane
535 concentrations in the context of the stabilization of greenhouse gas concentrations. *Journal of*
536 *Geophysical Research: Atmospheres*, 104, D16: 19183–19190, 1999.

537

538 Krasnopolsky, V. M., Fox-Rabinovitz, M. S., and Chalikov, D. V.: New approach to calculation
539 of atmospheric model physics: Accurate and fast neural network emulation of long wave
540 radiation in a climate model, *Mon. Weather Rev.*, 133, 1370–1383, 2005.

541

542 Krasnopolsky, V. M., and Fox-Rabinovitz, M. S.: Complex hybrid models combining
543 deterministic and machine learning components for numerical climate modeling and weather
544 prediction, *Neural Networks*, 19, 122–134, 2006.

545

546 Krasnopolsky, V. M., Fox-Rabinovitz, M.S., and Belochitski, A. A.: Using ensemble of neural
547 networks to learn stochastic convection parameterizations for climate and numerical weather
548 prediction models from data simulated by a cloud resolving model. *Adv. Artif. Neural. Syst.*, 1–
549 13, 2013.

550

551 Krasnopolsky, V. M., S. Nadiga, A. Mehra, E. Bayler, and D. Behringer: Neural networks
552 technique for filling gaps in satellite measurements: Application to ocean color observations,
553 *Computational Intelligence and Neuroscience*, 2016, Article ID 6156513, 9 pages, 2016.
554 doi:10.1155/2016/6156513

555

556 Krasnopolsky, V. M., J. Middlecoff, J. Beck, I. Geresdi, and Z. Toth. A neural network emulator
557 for microphysics schemes. 97th AMS annual meeting, Seattle, WA. January 24, 2017.

558

559 Lee, L. A., Carslaw, K. S., Pringle, K. J., Mann, G. M., and Spracklen, D. V.: Emulation of a
560 complex global aerosol model to quantify sensitivity to uncertain parameters, *Atmos. Chem.*
561 *Phys.*, 11, 12,253–12,273, 2011.

562

563 Leeds, W. B., Wikle, C. K., Fiechter, J., Brown, J., and Milliff, R. F.: Modeling 3D spatio-
564 temporal biogeochemical processes with a forest of 1D statistical emulators. *Environmetrics*,
565 24(1): 1–12, 2013.

566

567 McFarlane, N.: Parameterizations: representing key processes in climate models without
568 resolving them. *Wiley Interdisciplinary Reviews: Climate Change*, 2 (4): 482–497, 2011.

569

570 Scher, S.: Toward data-driven weather and climate forecasting: Approximating a simple general
571 circulation model with deep learning. *Geophysical Research Letters*, 45, 12,616–12,622, 2018.

572

573 Thompson, G., Field, P.R., Rasmussen, R.M., Hall, W.D.: Explicit forecasts of winter
574 precipitation using an improved bulk microphysics scheme. Part II: Implementation of a new
575 snow parameterization, *Mon. Weather Rev.* 136, 5095–5115, 2008.

576

577 Wang, J., and Kotamarthi, V. R.: Downscaling with a nested regional climate model in near-
578 surface fields over the contiguous United States, *Journal of Geophysical Research, Atmosphere*,
579 119, 8778–8797, 2014.

580

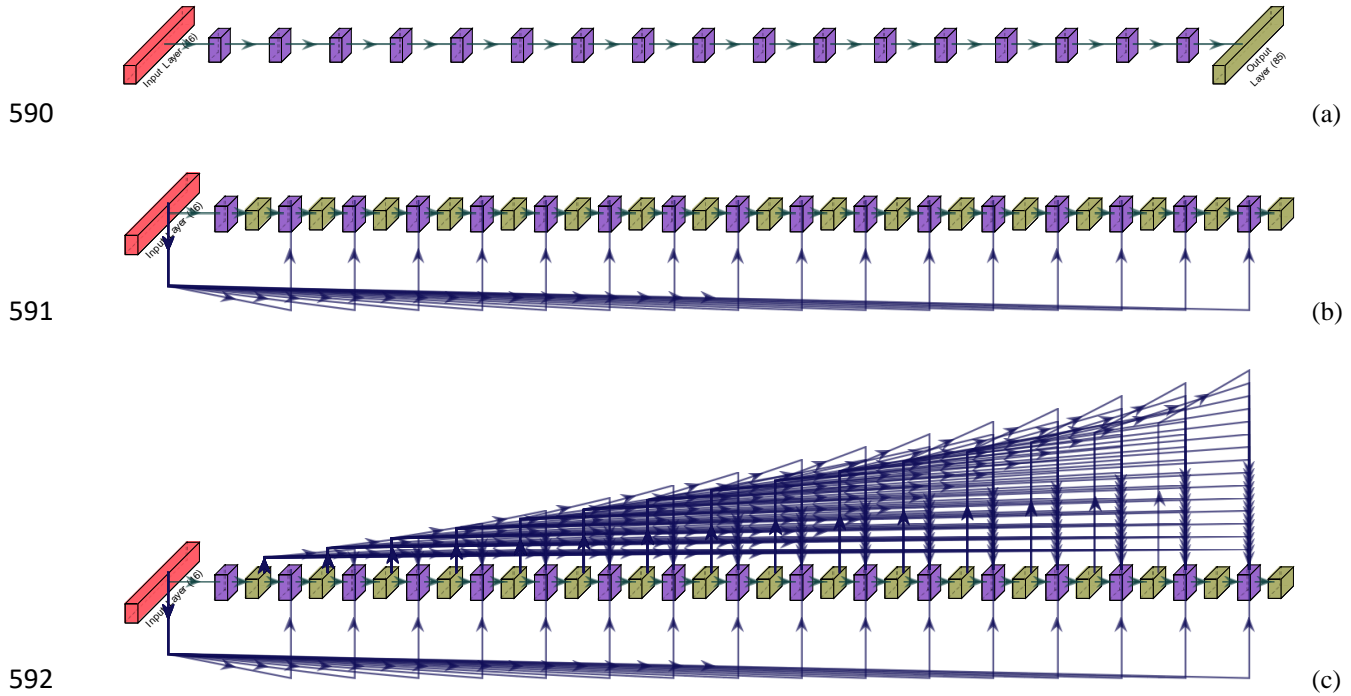
581 Williams, P. D.: Modelling climate change: the role of unresolved processes. *Philosophical*
582 *Transactions of the Royal Society A: Mathematical, Physical and Engineering Sciences* 363
583 (1837): 2931–2946, 2005.

584 **Table 1: Inputs and outputs for the NN developed in this study. The variable names of**
 585 **these inputs and outputs in the WRF are shown in the parentheses.**

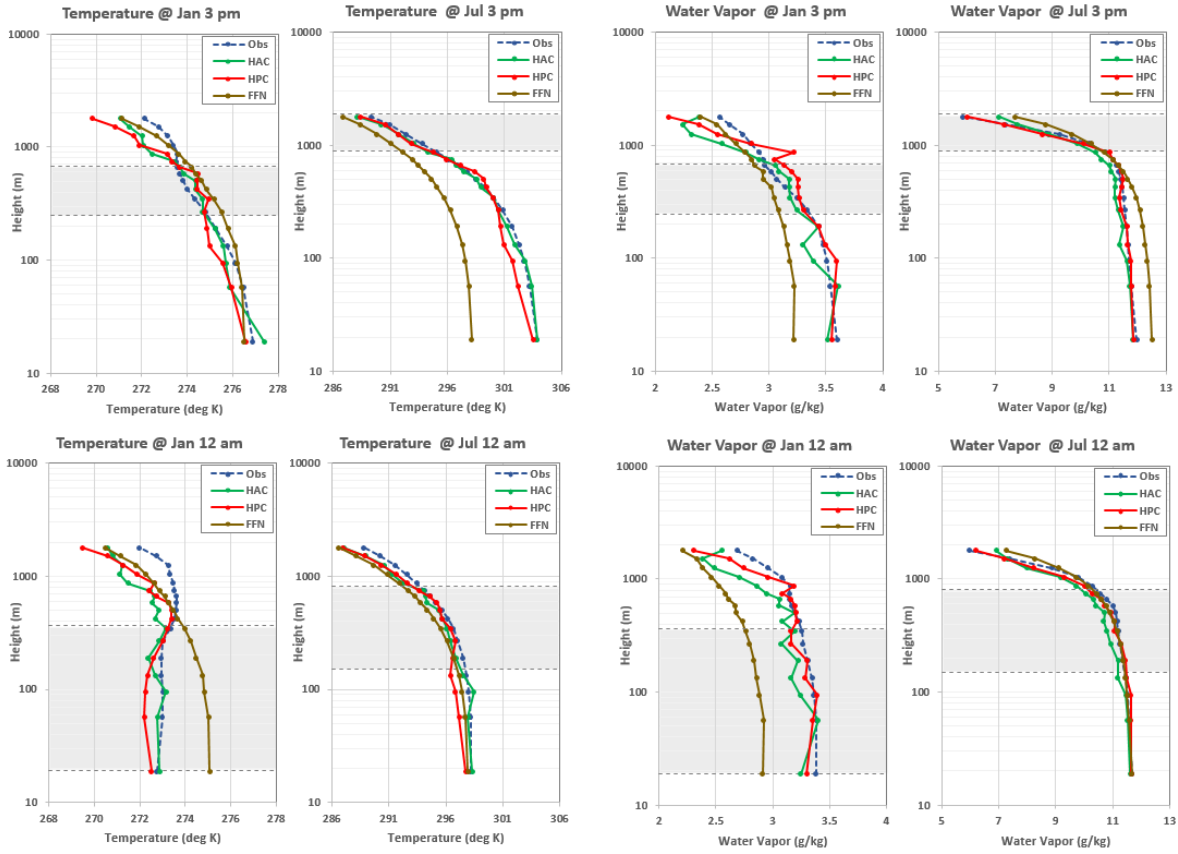
Input Variable	Output Variable
2-meter water vapor mixing ratio (Q2),	zonal wind (U)
2-meter air temperature (T2),	meridional wind (V)
10-meter zonal and meridional wind (U10, V10)	temperature (tk)
Ground heat flux (GRDFLX)	water vapor mixing ratio (QVAPOR)
Downward short wave flux (SWDOWN)	
Downward long wave flux (GLW)	
Latent heat flux (LH)	
Upward heat flux (HFX)	
Planetary boundary layer height (PBLH)	
Surface friction velocity (UST)	
Ground temp (TSK)	
Soil temperature at 2 m below ground (TSLB)	
Soil moisture for 0-0.3cm below ground (SMOIS)	
Geostrophic wind component at 700 hPa (Ug, Vg)	

587 **Table 2: Training and prediction time (unit: seconds) for the three DNNs using different**
 588 **lengths of training data. The predicted period is for one year (2005).**

DNN Type	Training Data (years)	Training Time (s)	Number of Epochs	Training Time (s) per Epoch	Prediction Time (s) for 1 Year (2005)
FNN	1	85.969	61	1.409	0.197
FNN	2	137.359	47	2.923	0.196
FNN	6	376.209	70	5.374	0.171
FNN	12	199.468	23	8.673	0.193
FNN	20	306.665	27	11.358	0.199
HPC	1	199.152	178	1.119	0.336
HPC	2	454.225	91	4.991	0.343
HPC	6	1233.908	133	9.278	0.317
HPC	12	1225.880	88	13.930	0.302
HPC	20	1181.716	68	17.378	0.331
HAC	1	131.104	95	1.380	0.366
HAC	2	468.884	85	5.516	0.411
HAC	6	870.753	80	10.884	0.406
HAC	12	737.921	47	15.700	0.420
HAC	20	1351.898	69	19.593	0.381

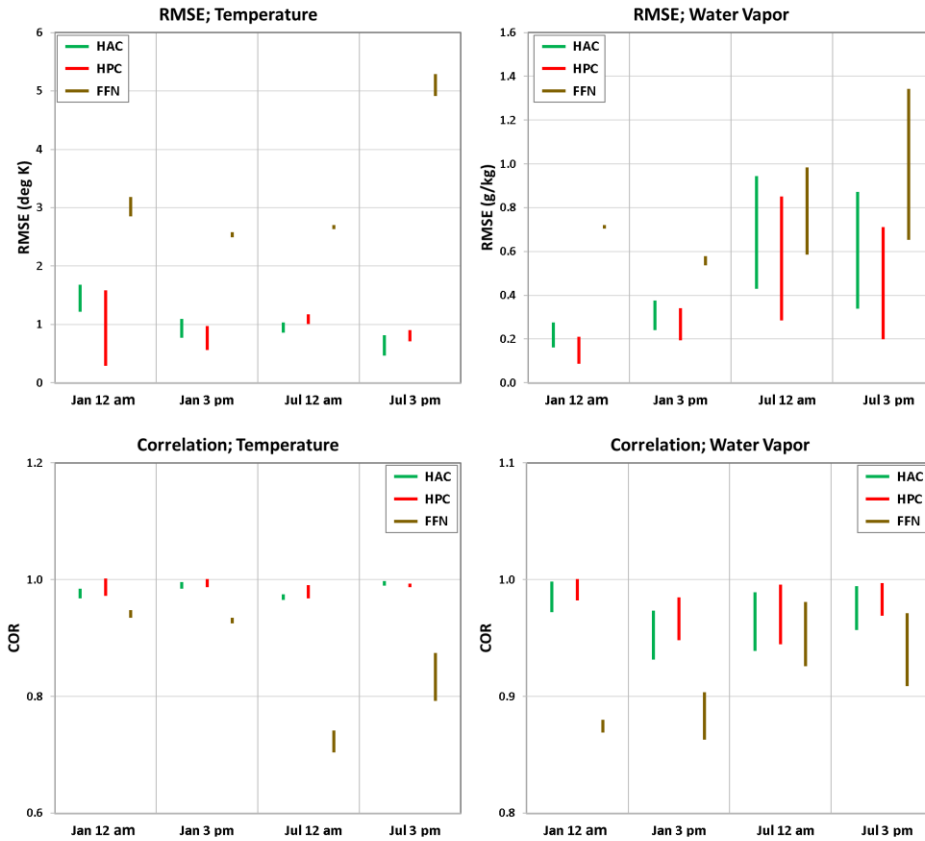


593 **Figure 1: Three variants of DNN developed in this study. Red, yellow, and purple indicate**
 594 **the input layer (16 near-surface variables), output layers, and hidden layers, respectively.**
 595 **(a) fully connected feed forward neural network (FFN), which has only one output layer**
 596 **with 85 variables (5 variables for each of the 17 WRF model vertical levels), and 17 hidden**
 597 **layers which only consider the near-surface variables as inputs.** (b) **hierarchically**
 598 **connected network with previous layer only connection (HPC), which has 17 output layers**
 599 **(corresponding to the PBL levels) with each of them having 5 variables, and 17 hidden**
 600 **layers with each them considering both near-surface variables and output variables from**
 601 **previous output layer as inputs.** and (c) **hierarchically connected network with all previous**
 602 **layers connection (HAC), same as HPC, but each hidden layer also considers output**
 603 **variables from all previous output layers as inputs.**



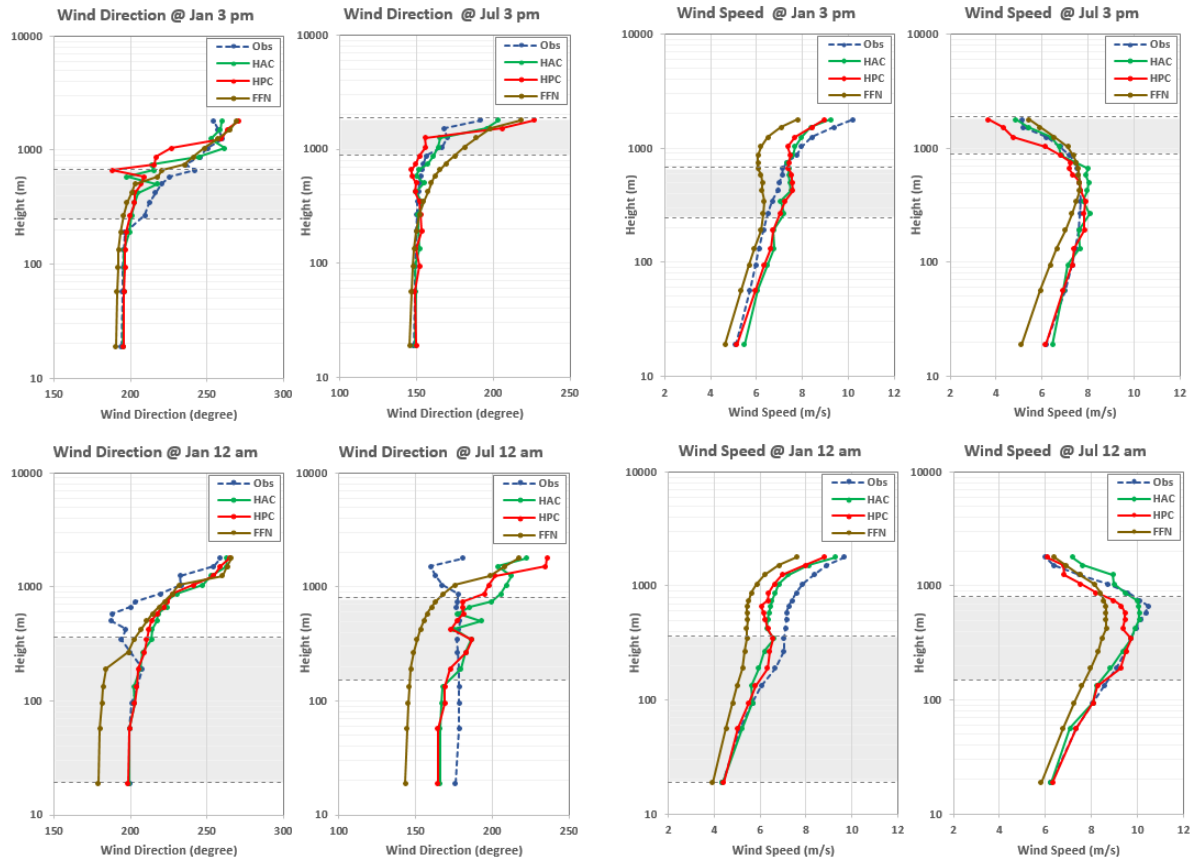
604

605 **Figure 2: Temperature and water vapor mixing ratio from the observation and three DNN**
 606 **predictions: FFN, HPC, and HAC in January and July of 2005 at 3 PM and 12 AM local**
 607 **time. The y-axis uses log scale. The training data are from 20 years (1984 to 2003) of 3-**
 608 **hourly WRF output. The lower and upper dash lines show the lowest and highest (5th and**
 609 **95th percentile) PBL heights at that particular time. For example, in January 12 AM, the**
 610 **lowest PBL height is about 19 m, while the highest PBL height is about 365 m.**



611

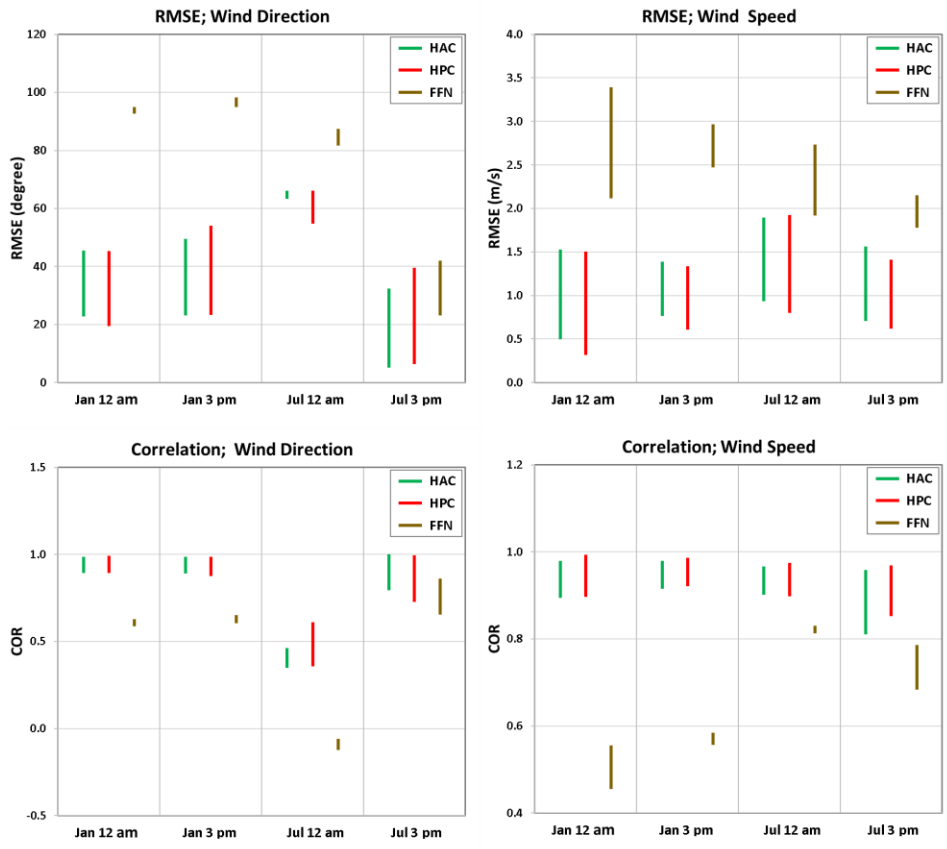
612 **Figure 3: RMSE and correlations for time series of temperature and water vapor vertical**
 613 **profiles within the PBL predicted by the three DNNs compared with the observations. The**
 614 **vertical lines show the range of RMSEs and correlations when considering the lowest and**
 615 **highest PBL heights at each particular time (shown by the dashed horizontal lines in**
 616 **Figure 2). The training data are 3-hourly WRF output from 1984 to 2003.**



617

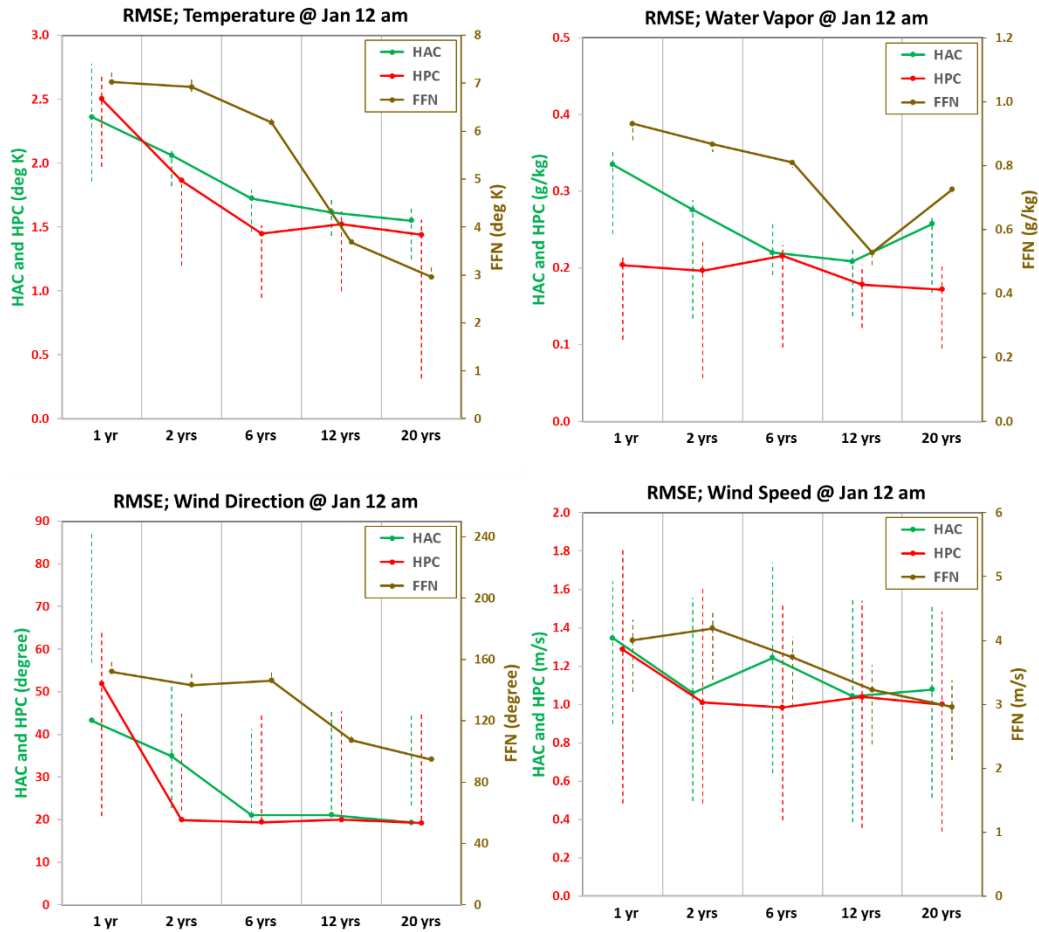
618

Figure 4: Same as Figure 2 but for wind direction and wind speed.



619

620 **Figure 5: Same as Figure 3 but for wind components.**



621

622

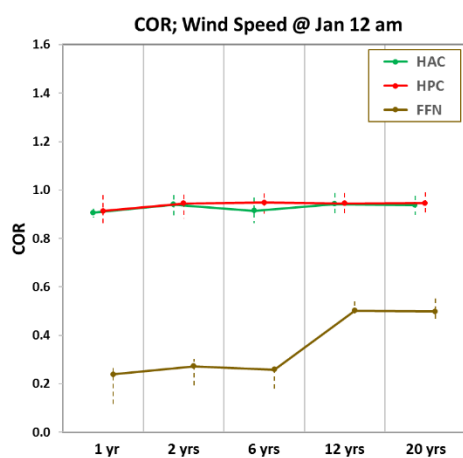
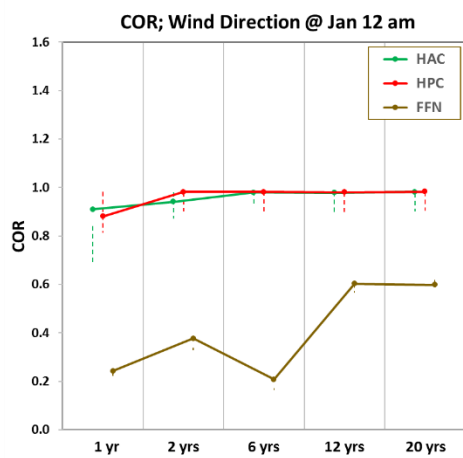
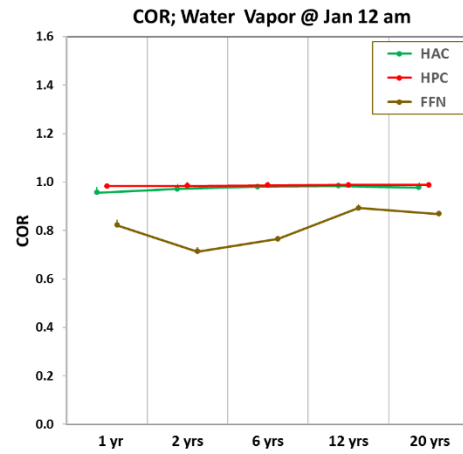
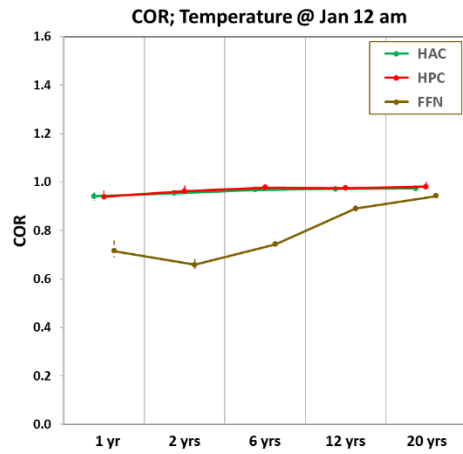
623

624

625

626

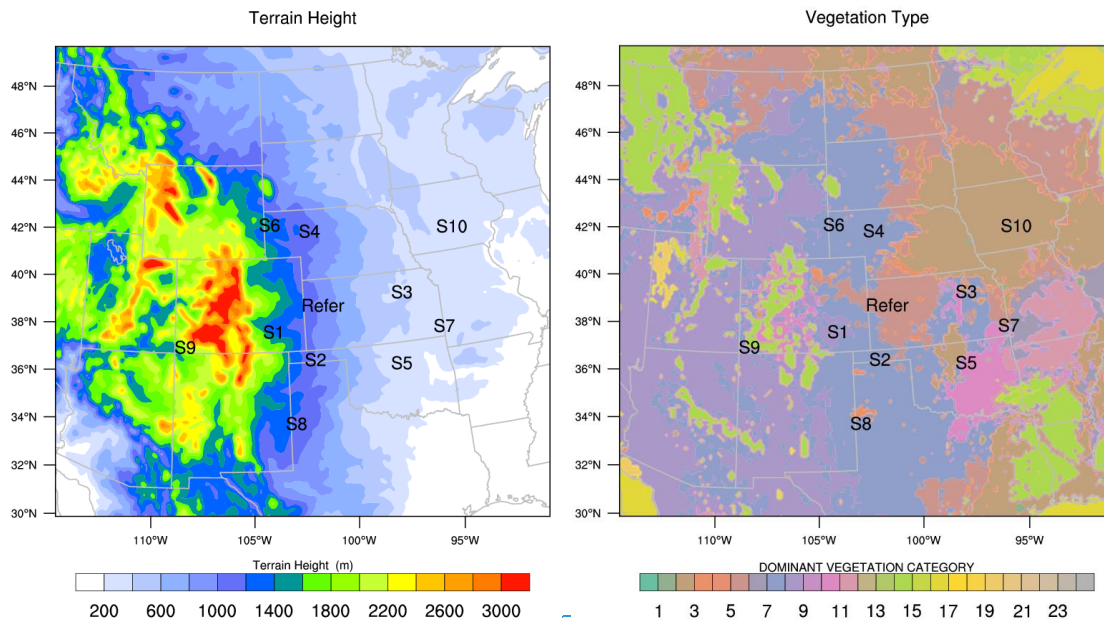
Figure 6: RMSEs for temperature, water vapor, and wind components at midnight of January using three DNNs. Left y-axis is for RMSEs of HAC and HPC; right y-axis is for RMSE of FFN. The RMSEs are calculated along the time series below the PBL height for January midnight at local time. The lower and upper end of the dash lines are RMSEs that consider the lowest and highest PBL heights as shown in Figure 2.



627

628

Figure 7: Same as Figure 6 but for Pearson correlations.

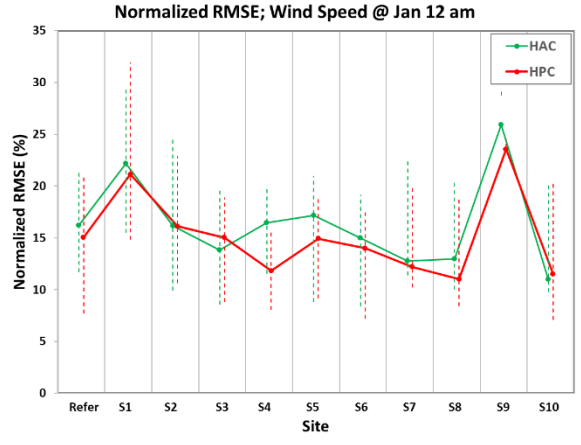
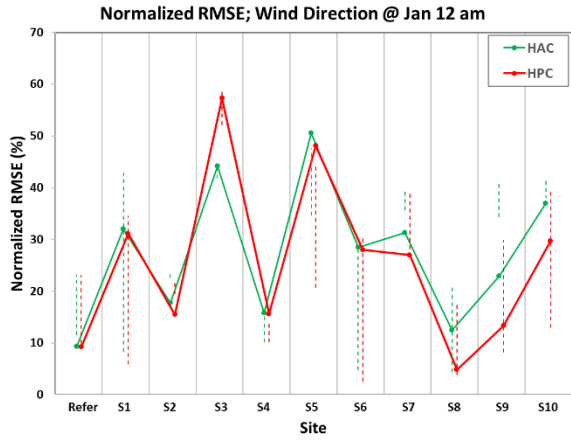
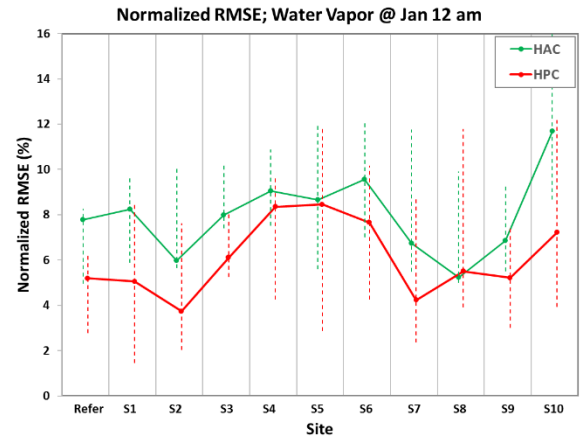
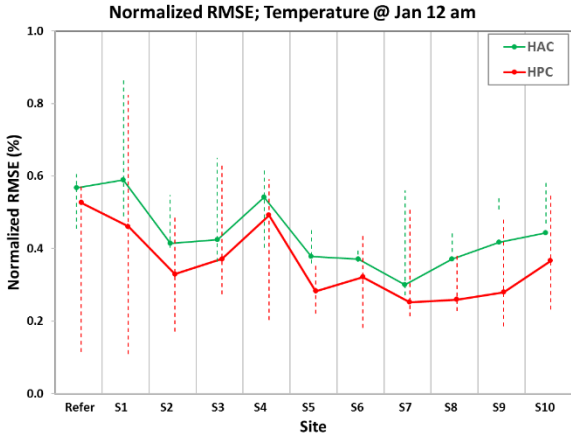


629

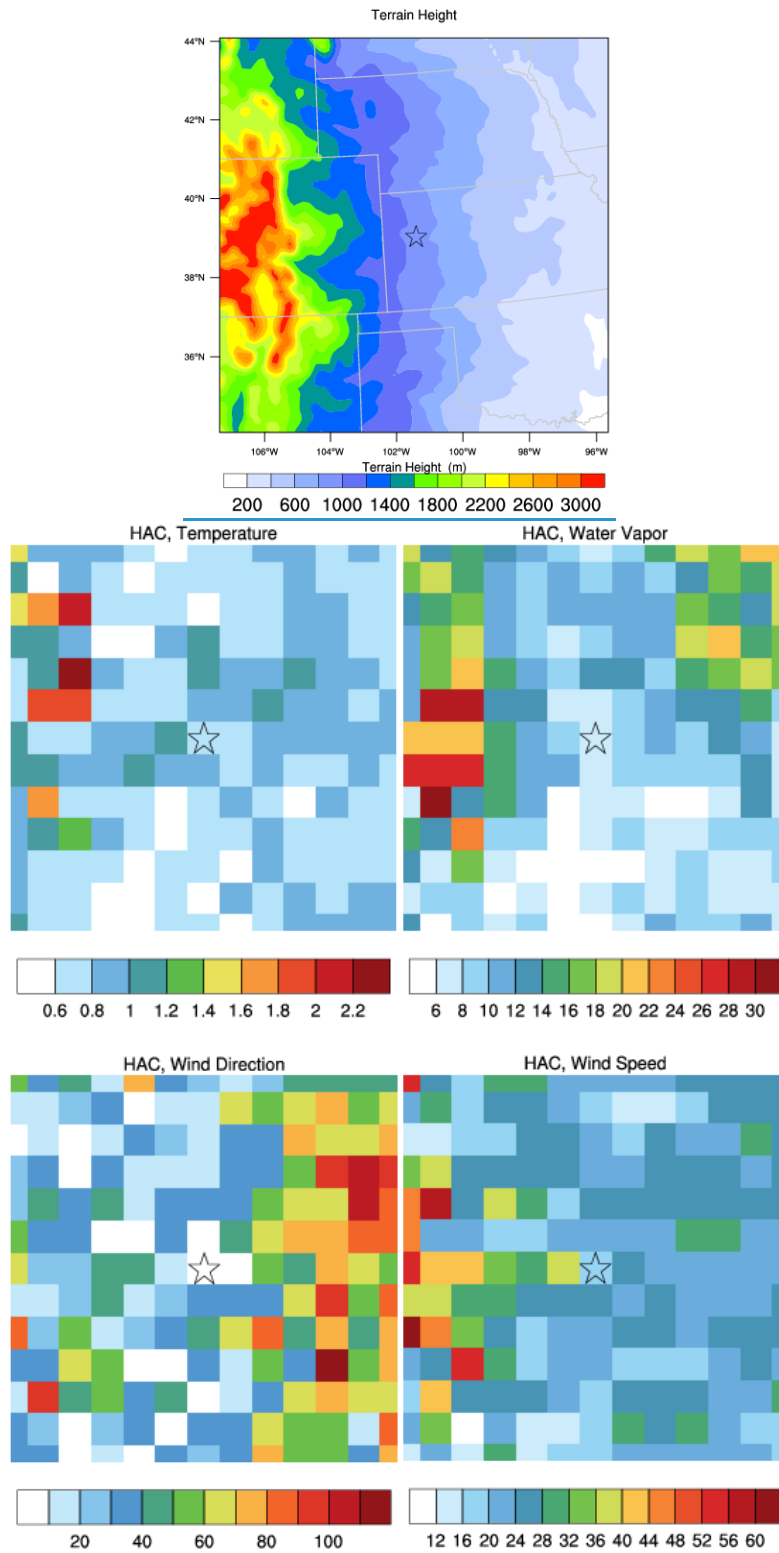
630

631

Figure 8: Terrain height (left) and vegetation types (right) for Logan, Kansas, and other locations that we used to assess the spatial transferability of our domain-aware DNNs.



633



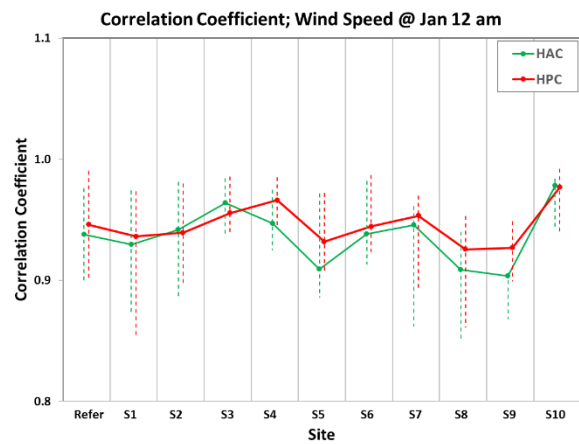
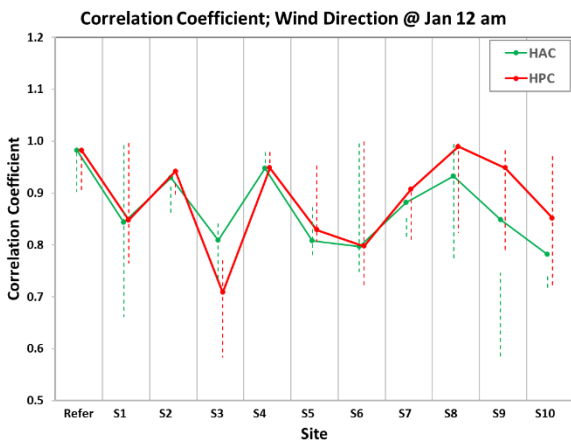
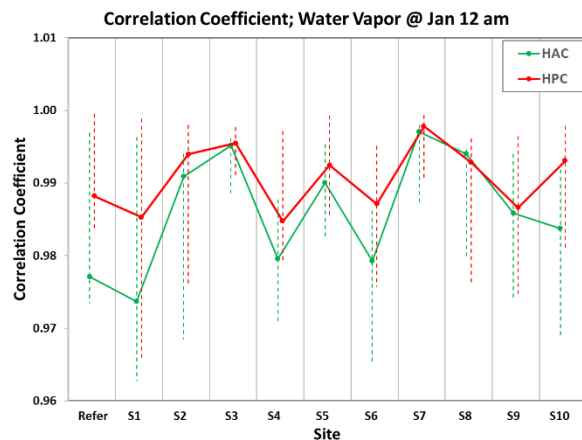
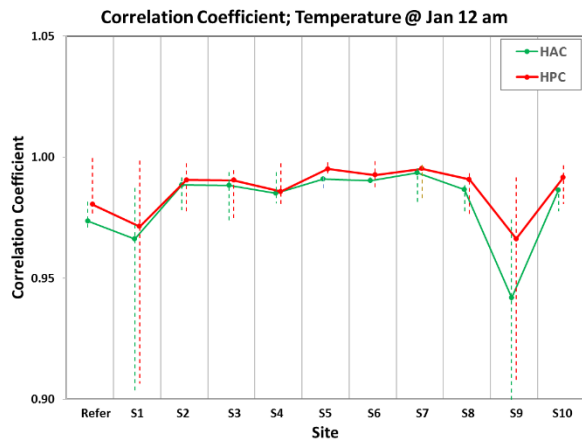
634

635

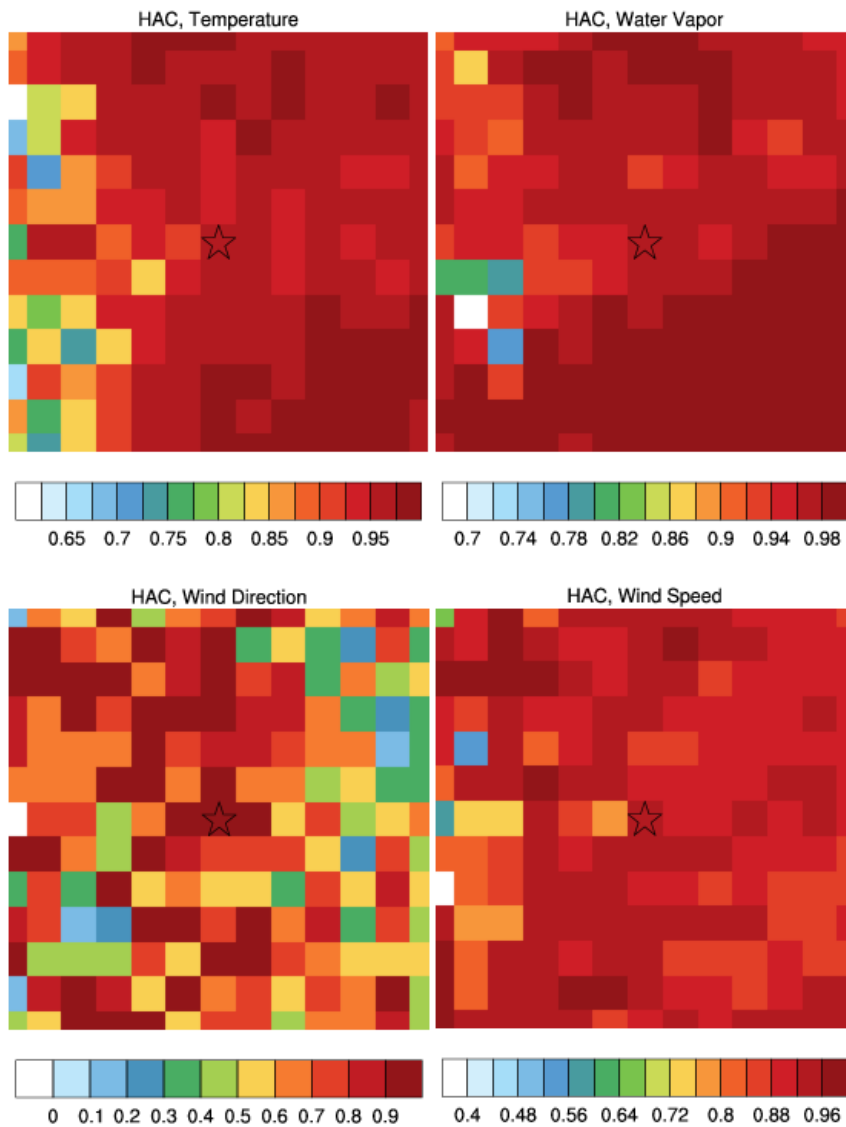
636

Figure 98: Terrain height (in meters) over the tested area; and N ormalized RMSEs in % (relative to their corresponding observations) of HAC predicted relative to their

637 corresponding observations at midnight of January for temperature, water vapor mixing
 638 ratio, and wind direction and speed component at midnight of January. The star shows
 639 where the DNNs are developed sites are in the order of short to long distance from the
 640 reference site at (Logan, Kansas).



641



642

643 **Figure 109: Same as Figure 9 but for Person correlations between observed and HAC DNN**
 644 **predictions temperature, water mixing ratio, wind direction and speed for midnight of**
 645 **January in 2005 and observations.**